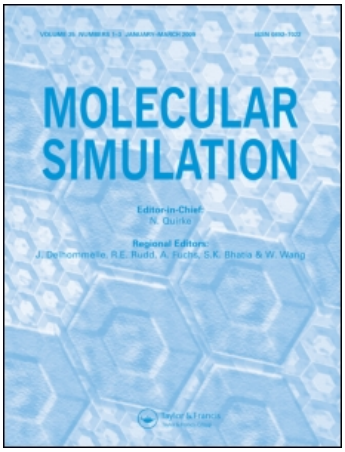

Molecular Simulation
Publication details, including instructions for authors and subscription information:
http://www.informaworld.com/smpp/title~content=t713644482

Ab-initio simulations of magnetic iron sulphides

S. Wells[a]; D. Alfe[b]; L. Blanchard[c]; J. Brodholt[b]; M. Calleja[d]; R. Catlow[a]; D. Price[b]; R. Tyler[c]; K. Wright[a]
[a] Royal Institution, London, UK [b] Department of Earth Sciences, University College, London, UK [c] CCLRC Daresbury, Cheshire, UK [d] Department of Earth Sciences, University of Cambridge, Cambridge, UK

To cite this Article Wells, S. , Alfe, D. , Blanchard, L. , Brodholt, J. , Calleja, M. , Catlow, R. , Price, D. , Tyler, R. and Wright, K.(2005) '*Ab-initio* simulations of magnetic iron sulphides', Molecular Simulation, 31: 5, 379 — 384
To link to this Article: DOI: 10.1080/08927020500066361
URL: http://dx.doi.org/10.1080/08927020500066361

Molecular Simulation, Vol. 31, No. 5, April 2005, 379–384

Taylor & Francis
Taylor & Francis Group

Ab-initio simulations of magnetic iron sulphides

S. WELLS†*, D. ALFE‡, L. BLANCHARD¶, J. BRODHOLT‡, M. CALLEJA§, R. CATLOW†, D. PRICE‡, R. TYLER§ and K. WRIGHT†

†Royal Institution, Albemarle Street, London W1S 4BS, UK
‡Department of Earth Sciences, University College, London, UK
¶CCLRC Daresbury, Cheshire, UK
§Department of Earth Sciences, University of Cambridge, Cambridge, UK

(Received July 2004; in final form September 2004)

We present the results of simulations, using density functional theory (DFT) with generalized gradient corrections (GGA), on the troilite (FeS), pyrrhotite ($Fe_{1-x}S$) and MnP phases of FeS. The values obtained for the cell parameters and *c/a* ratio of troilite accurate to within 1% of those determined by experiment, a significant improvement on previous simulations. Energy–volume curves for FeS in the troilite and MnP structures indicate a pressure-induced transition at 4 GPa (experimentally observed at 3.4 GPa). Comparison of spin-polarised and non-spin-polarised simulations of the troilite structure demonstrate the significance of magnetostructural effects in determining the *c/a* ratio and shed light on the magnetic and volume collapse of FeS on its transition from the MnP to a monoclinic structure at 6.7 GPa. Simulations of different (001) surface terminations of troilite indicate that stable surfaces are characterised by triangles of iron atoms "capped" with a sulphur atom.

Keywords: Density functional theory; Generalized gradient corrections; Troilite; Pyrrhotite

1. Introduction: environmental significance of iron sulphides

The Fe–S minerals are ubiquitous in nature, where they are associated with massive sulphide type ore deposits, as well as anaerobic sedimentary and exhalative volcanic environments. The stable phases in the Fe–S system are pyrite (cubic FeS_2) and the pyrrhotites ($Fe_{1-x}S$), although many metastable phases are known to exist including mackinawite (FeS_{1-x}) and greigite (Fe_3S_4). Stoichiometric FeS (troilite) is rare and normally only found in meteorites. Fe sulphides are important from an environmental perspective because of their high reactivity under oxidising conditions. Breakdown of pyrite and pyrrhotite leads to high acidity in surrounding waters, which in turn promotes further leaching and dissolution of other mineral phases. This phenomenon, known as acid rock (ARD) or acid mine drainage (AMD) can lead to the release of potentially toxic elements. In mine waste tailings this is of particular concern since Zn, Pb, Cu, Ni, Cd, Hg and As can all be released into the environment. The pyrrhotite group are some of the most common of the Fe–S minerals, and the most reactive [1]. Their composition and structure vary according to the number and degree of ordering of Fe vacancies, as do their magnetic properties [2]. For example, monoclinic pyrrhotite (Fe_7S_8) has an ordered defect structure and is weakly ferromagnetic, whilst hexagonal pyrrhotite ($Fe_{11}S_{12}$) is antiferromagnetic [3]. Observations, both in the field and the laboratory, have found that the breakdown of hexagonal and monoclinic pyrrhotite occurs at different rates. No clear reason for this has been put forward, since the field and laboratory data do not always agree on which is the most reactive phase [4]. The reaction rate will be related not only to the available surface area, but also to the atomic structure of the surface. Defect and magnetic properties at the surface may also influence reactivity.

Our aim is to simulate the bulk and surface structure of defective pyrrhotites in order to better understand the way in which defect ordering and magnetic properties influence their behaviour in the environment. As a first step, we have modelled stoichiometric FeS in the troilite structure in order to quantify the effects of magnetism on the cell parameters. We report our results on the troilite structure, its elastic properties, its pressure-induced transition to the MnP structure, and the significance of

*Corresponding author. E-mail: stephen.a.wells@asu.edu

Molecular Simulation
ISSN 0892-7022 print/ISSN 1029-0435 online © 2005 Taylor & Francis Group Ltd
http://www.tandf.co.uk/journals
DOI: 10.1080/08927020500066361

its magnetostructural effects. We also describe our work currently in progress on troilite surfaces and on ferromagnetic and antiferromagnetic bulk pyrrhotites.

This work is part of the larger NERC funded eMinerals project (www.eminerals.org) [5] and has made extensive use of the associated GRID resources detailed in this issue of *Molecular Simulation* [6] and elsewhere [7–9].

2. Previous simulation studies on troilite

Troilite has been previously investigated by Martin *et al.* [10], who studied the pressure-induced transitions in the FeS system using density functional theory (DFT)-generalized gradient corrections (GGA). They found that troilite transforms successively into the MnP structure, a monoclinic structure, and finally the CsCl structure with increasing pressure. The transitions to the MnP and monoclinic structures have been experimentally observed [11] while the CsCl structure is predicted to be stable at very high pressures. This work was the starting point for our investigation. We note that the *c/a* ratio for troilite was underestimated in this work by more than 4% (1.88 vs 1.97).

Hobbs and Hafner [12], in the course of a general investigation of the transition metal sulphides, used DFT-GGA with the projected augmented wave (PAW) formalism to simulate FeS in the troilite and NiAs structures. This work also underestimated the *c/a* ratio for troilite (table 1). Rohrbach *et al.* [13] investigated the transition metal sulphides using the LDA + U approach to account for the electronic correlation effects that are not properly considered using GGA. This work showed that, while it is possible to obtain better predictions of properties such as volume, magnetic moment and bandgap using the LDA + U approach, a different value of U is required to optimise each parameter.

3. Structure and properties of antiferromagnetic troilite

Our calculations have been carried out using version 4.6 of the VASP plane-wave DFT code† [16] in the Generalised Gradient Approximation using the PW91 functional and the spin interpolation for the exchange-correlation energy of Vosko *et al.* [17]. Brillouin-zone integrationwas performed using the Gaussian smearing [18] Monkhorst-Pack (MP) special point [19] technique. We found that energies were converged to one part in 10^6 by using a $6 \times 6 \times 4$ grid and a first order Gaussian smearing function [18] of width sigma = 0.2 eV. A plane wave cutoff of 500 eV was used throughout.

Troilite has the hexagonal structure shown in figure 1, with space group (P -6 2 *c*) and 24 atoms in the unit cell.

Table 1. Comparison of experimental and calculated values of cell parameters and *c/a* ratio for troilite

Investigation	*a* (Å)	*c* (Å)	*c/a ratio*
AFM this study	5.953	11.66	1.96 (0.5%)
NM this study	5.858	10.47	1.79 (9%)
AFM Martins *et al.* [10]	5.981	11.232	1.88 (4.5%)
AFM Hobbs and Hafner [12]			1.83 (7%)
NM Hobbs and Hafner [12]			1.79 (9%)
Troilite, experimental [15]	5.966(1)	11.76(1)	1.97
Troilite, experimental [11]	5.963(1)	11.754(1)	1.97

Values in brackets represent difference from experiment. AFM = antiferromagnetic, NM = nonmagnetic.

The magnetic moments of the Fe atoms are aligned parallel to the c axis and are antiferromagnetically ordered, with alternating layers of iron atoms along the *c* direction having oppositely aligned moments, as given by Martin *et al.* [10]. The structure is a slight distortion of the NiAs structure and is apparently unique to FeS. We present our calculated cell parameters in table 1 and atomic coordinates in table 2, where comparison is given with experiment and with previous theoretical studies. We find that our simulation of the magnetic structure gives values of a, c and the ratio *c/a* within 1% of experimental values and represents a significant improvement over previous simulations.

Perhaps the most striking feature of these results is that shown by comparison of the AFM and NM structures. Simulation of the nonmagnetic troilite structure shows a dramatic collapse of the c axis causing an ~10% decrease in the volume per formula unit, illustrating the magnitude of the magnetostructural effects in this mineral. We note that the transition from the MnP-type structure (antiferromagnetic) to the monoclinic structure (nonmagnetic) at 6.7 GPa [11] is reported to involve a very similar collapse of the c_{troilite} axis with disappearance of the magnetic moment [14]. This leads us to conclude that magnetic interactions are crucial in determining the *c/a* ratio for FeS, and that the underestimation of *c/a* in previous simulations [10,12] may be related to the handling of magnetism.

A graph of energy versus volume per formula unit for FeS in the antiferromagnetic and nonmagnetic troilite structures is given in figure 2. The fitted line is for a third-order Birch-Murnaghan equation of state for magnetic troilite. Our value for the bulk modulus *K* of 74.0 GPa is consistent with previous simulations and with experiment. We have also simulated uniaxial compression of the magnetic troilite structure in the *c* direction; figure 3 shows the variation of the unit cell energy with variation of the *c* axis. The fitted line corresponds to an elastic constant c_{33} of 158 GPa. The values computed in this study are compared with those from experiment and from the simulations of Martin *et al.* in table 3.

†VASP webpage at http://cms.mpi.univie.ac.at/vasp/

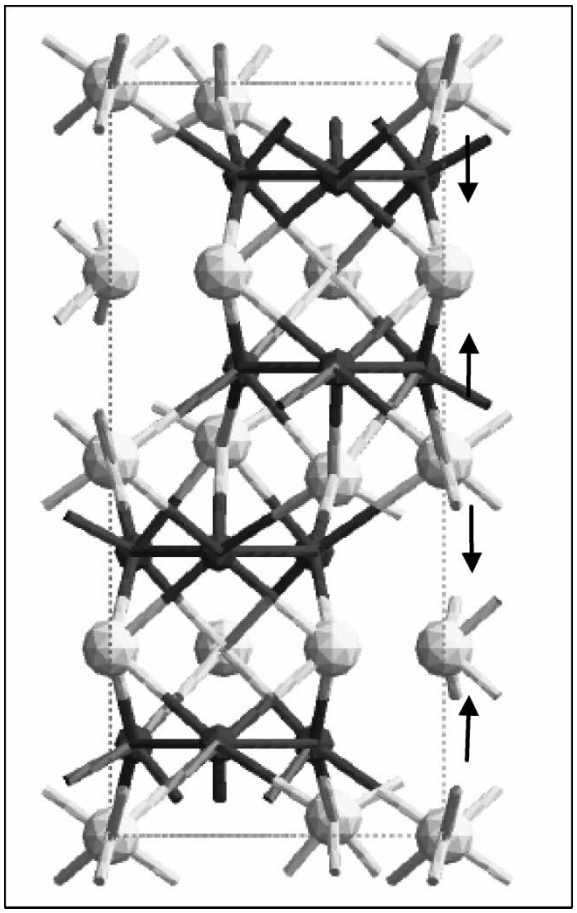

Figure 1. Structure of troilite viewed normal to *c*. Arrows show antiferromagnetic ordering of Fe ions.

4. Troilite to MnP-structure phase transition

We have used CSAR resources to simulate FeS in the MnP structure, using similar settings as for troilite, and a $7 \times 7 \times 7$ k-point grid. Several possible antiferromagnetic arrangement of the iron moments are possible in the MnP structure; on simulation of all three arrangements, we obtain the lowest energy for the same pattern as given by Martin *et al.* [10], in which moments are ordered in layers along the a_{MnP} axis.

Table 2. Calculated and experimental atomic coordinates for troilite

Fe positions	*X*	*Y*	*Z*
A	0.3787(2)	0.0553(2)	0.12300(9)
B	0.3943	0.0727	0.12044
C	0.39183	0.07031	0.12177
S positions			
A	0	0	0
	0.333333	0.666667	0.0208(2)
	0.6648(6)	−0.0041(4)	0.25
B	0	0	0
	0.333333	0.666667	0.0278
	0.6641	0.0066	0.25
C	0	0	0
	0.333333	0.666667	0.02431
	0.66343	0.00029	0.25

A = King and Prewitt [11]; *B* = Martin *et al.* [10]; *C* = This work.

Our results for the MnP structure, with comparison to the results of Martin *et al.* and to experimental results, are given in table 4. Figure 4 indicates that the MnP structure becomes more stable than the troilite structure at a volume per formula unit of 28.09 Å^3, at an energy per formula unit of − 13.21 eV. The change in energy per unit volume between these values, and the values of E_0 and V_0 for troilite, corresponds to a pressure of 3.99 GPa for the transition between troilite and the MnP structure at zero *K*. The transition occurs experimentally at 3.4 GPa [11] at room temperature; the difference between the experimental and theoretical results may indicate the influence of temperature.

5. Troilite surfaces

Having investigated the bulk properties of troilite, we are now considering its surfaces, beginning with (001). This surface is both significant crystallographically and amenable to investigation. Calculations using VASP with a 500 eV plane-wave cutoff and a $6 \times 6 \times 1$ k-point grid, using the smearing method of Methfessel and Paxton [18], show that convergence of the vacuum gap is achieved at 12 Å. Comparison of forces for slabs of different thicknesses shows good convergence of forces even for a slab only one cell thick. We have, therefore, begun by investigating the surface reconstructions observed in slabs of single-cell thickness.

When examined in detail, the bulk structure is characterised by a motif of iron "prisms", "capped" on their triangular and square faces by sulphur atoms, as shown in figure 5. This suggests that the stability of troilite surfaces will depend on whether this motif is preserved.

We compare two slabs, one produced by a simple truncation of the unit cell (slab *A*) (figure 6a) and one produced by a subsequent relocation of two sulphur atoms so as to preserve the sulphur "capping" of the iron "prisms" that characterises the bulk structure (slab *B*) (figure 6b). On relaxation, the average surface energy for the surfaces of slab *A* is 1.068 J/m^2 and that for slab *B* is 0.859 J/m^2. The lower surface of slab *A* (figure 6c) reconstructs so as to recreate the "capped" structure, confirming the significance of this motif in producing stable surfaces. Slab B retains the "capped" structure on both surfaces and shows a lower surface energy. This suggests that the most stable surfaces of troilite and pyrrhotite will be those that retain the "capped" structure, while those that lack this structure, due for example to the presence of an iron vacancy defect, will be less stable and thus more vulnerable to dissolution. This may well be relevant to the differential rates of dissolution for pyrrhotites with different iron vacancy structures.

6. Further work

The calculations reported in this paper are the first steps towards environmentally relevant simulations of iron sul-

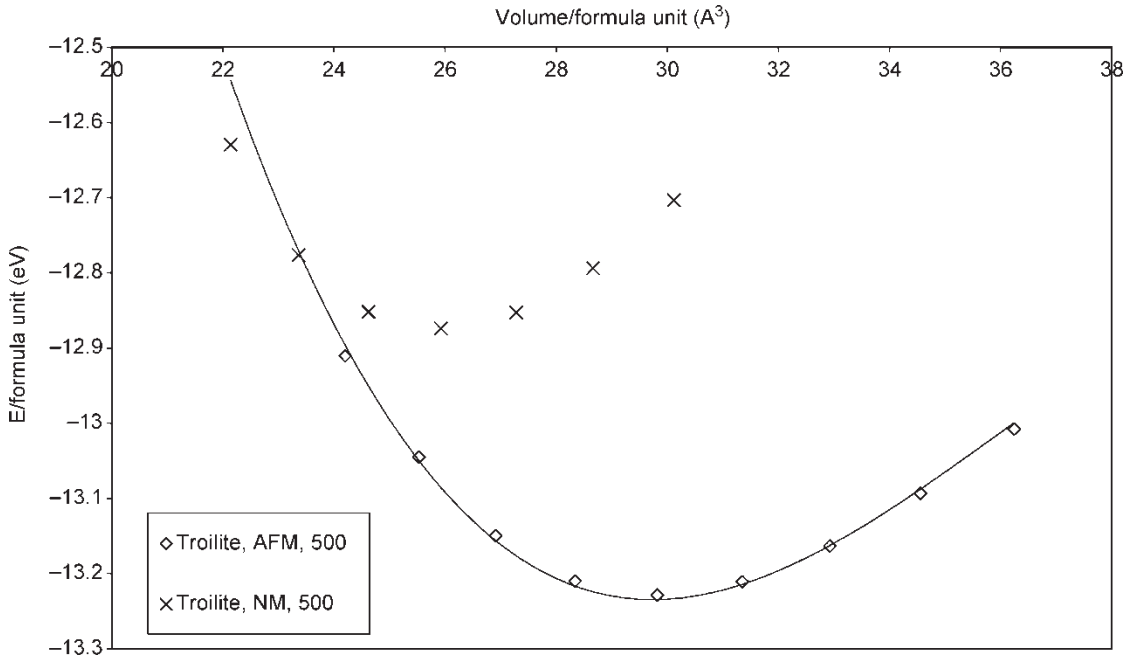

Figure 2. Energy versus volume per formula unit for magnetic and nonmagnetic troilite; note the dramatic collapse of the nonmagnetic structure. The fitted line is a 3rd-order Birch-Murnaghan equation of state.

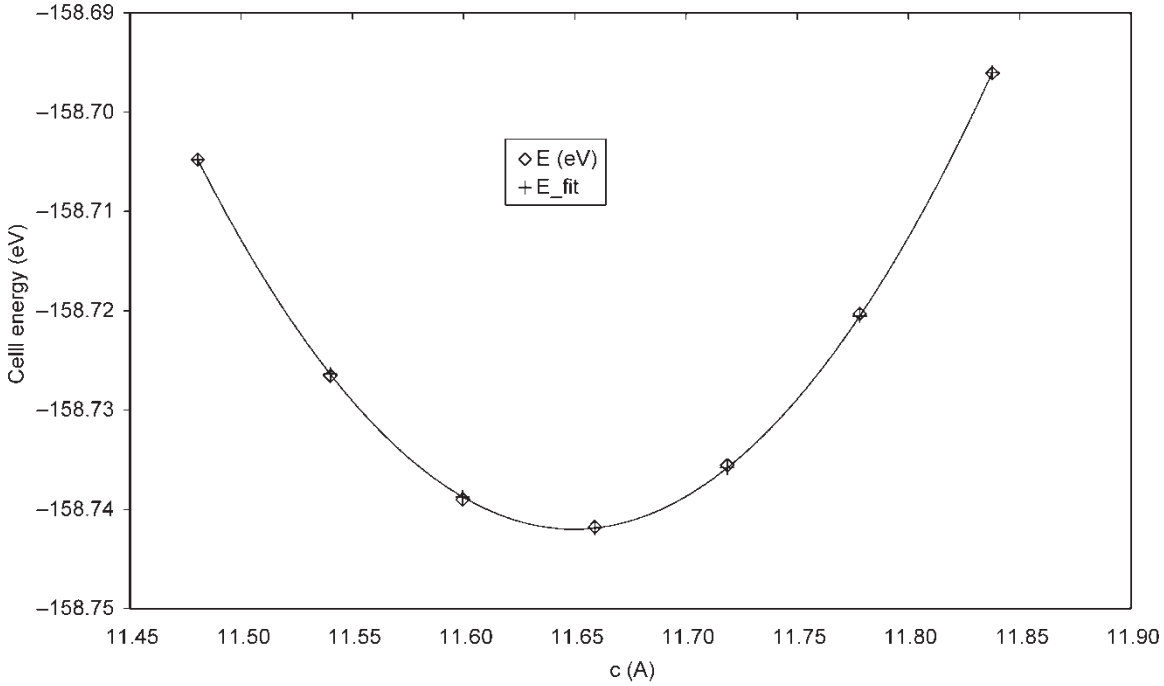

Figure 3. Uniaxial compression of troilite with fitted elastic constant c_{33}.

Table 3. Third-order Birch-Murnaghan equations of state for troilite

Investigation	V_0 (Å^3)	E_0 (eV)	K (Gpa)	K'
AFM this study	29.714	−13.231	74	3.770
AFM Martin *et al.* [10]	29.06(2)	−13.0677(4)	75.6(7)	−0.9(2)
Troilite, experimental [15]			73(3)	
Troilite, experimental [11]	30.16(9)		82(7)	−5(4)

Table 4. Third-order Birch-Murnaghan equations of state for MnP-structured FeS

Investigation	V_0 (Å^3)	E_0 (eV)	K (GPa)	K'
Our simulation	28.731	−13.208	74	3.825
Simulation [10]	27.84(1)	−13.0641(2)	76.8(3)	2.20(9)
Experimental [15]	26.89		44(3)	
Experimental [11]	28.2(3)		35(4)	5(2)

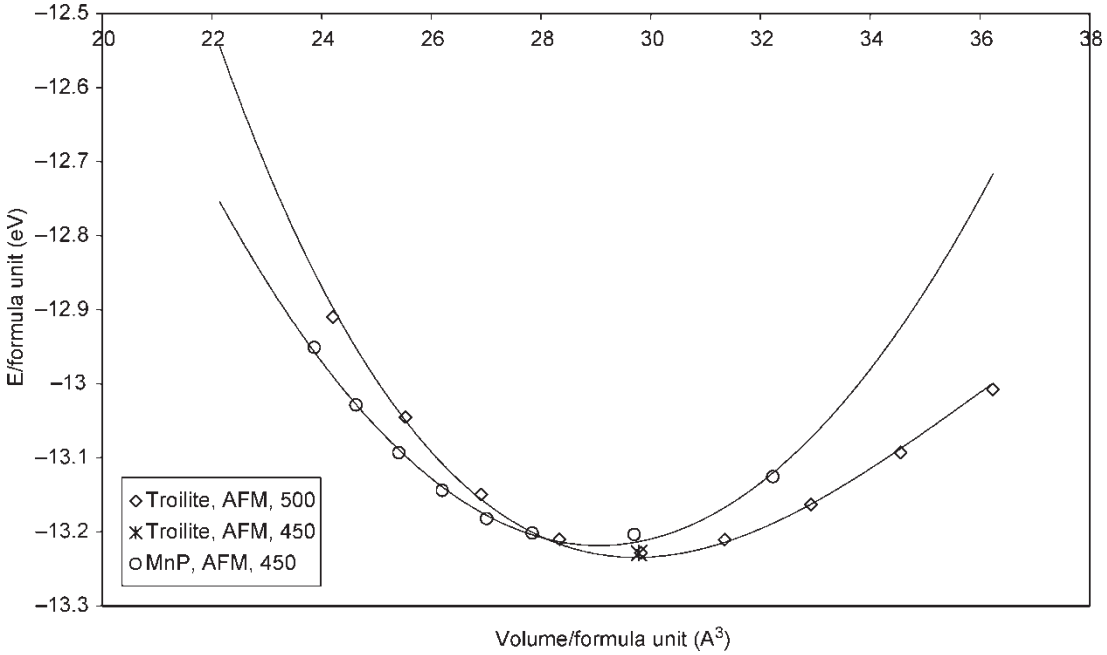

Figure 4. Energies versus volume per formula unit for troilite and MnP structures of magnetic FeS. Troilite data calculated using the 450 eV cutoff were consistent with those using the 500 eV cutoff. Fitted lines are 3rd-order Birch-Murnaghan equations of state.

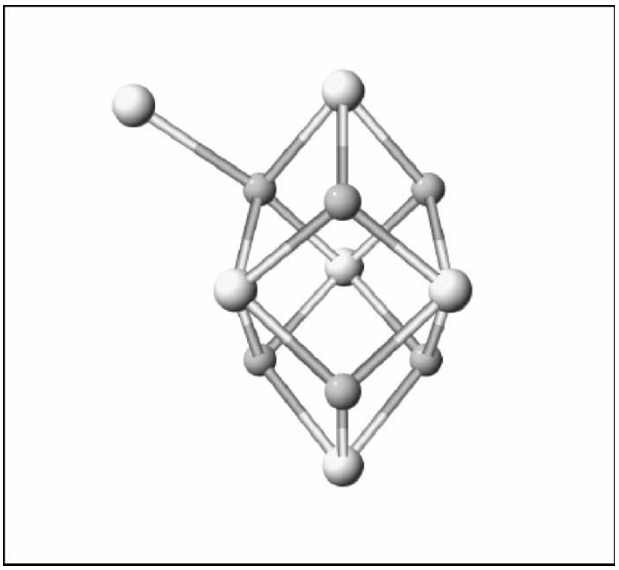

Figure 5. The bulk structure of troilite contains these triangular prisms of iron atoms, "capped" by sulphur. The appended sulphur atoms is at the high-symmetry position (0,0,0) in the cell.

phides. Currently, we are working towards the determination of the magnetostructural effects in stocihiometric and non-stoichimetric pyrrhotite phases. These simulations are particularly demanding because of the large unit cell sizes (more than 100 atoms). Our preliminary simulations indicate that inclusion of magnetism for Fe_7S_8 pyrrhotite is necessary to correctly describe the structure. In addition to the above, we are carrying out a detailed investigation of the low index surfaces of FeS which will be the subject of a future paper.

7. Conclusions

DFT simulations of magnetic troilite using GGA at very high accuracy provide an accurate simulation of the equilibrium structure and elastic properties of troilite, attaining higher accuracies (within 1% of experiment) than those obtained in previous studies. Comparison of the structures of magnetic and non-magnetic pyrrhotite, and of the experimentally observed volume collapse in FeS on transition from the MnP to a monoclinic structure, indicate

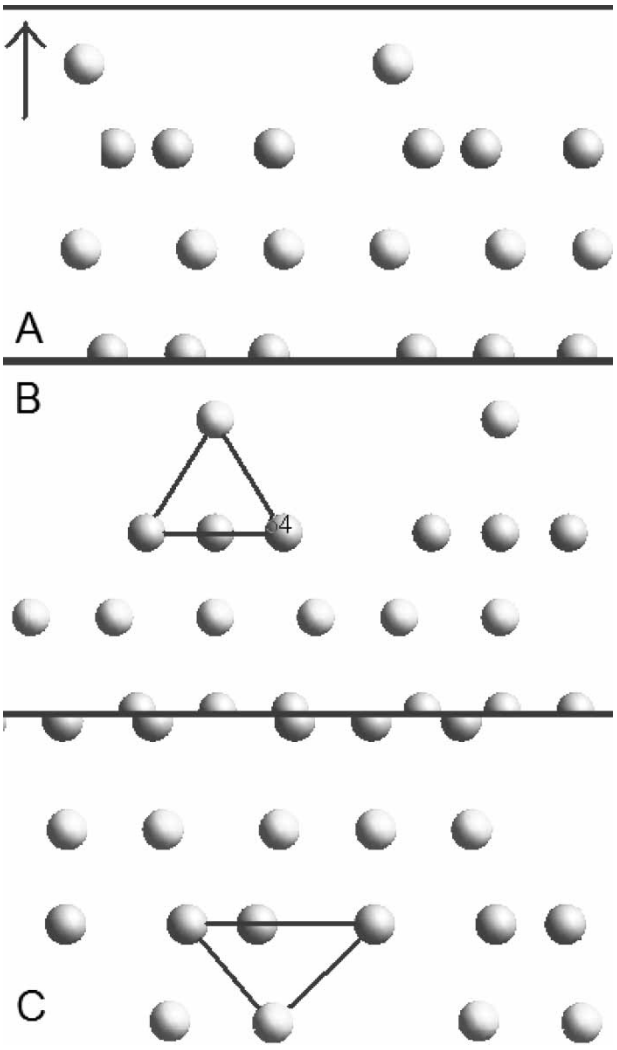

Figure 6. (a) upper surface of slab *A*, (b) upper surface of slab *B*, showing capped-prism motif (c) lower surface of slab *A*, showing recreation of capped-prism motif.

that magnetic interactions are critical in determining the *c*/*a* ratio for troilite.

Acknowledgements

This work has been funded by the NERC as part of the eMinerals project. SAW would like to thank Dr Georg Kresse and others of the VASP group at Vienna University for training in the use of the VASP code.

References

[1] H.W. Nesbitt, J.L. Jambor. Role of mafic minerals in neutralizing ARD, demonstrated using a chemical weathering methodology. In *Modern Approaches to Ore and Environmental Mineralogy*, L.J. Cabri, D.J. Vaughan (Eds.), Min Soc of Canada Short Course Series **27**, pp. 403–421 (1998).

[2] D.J. Vaughan, J.R. Craig. *Mineral Chemistry of Metal Sulphides*, Cambridge University Press, Cambridge, UK (1978).

[3] A.R. Lennie, K.E.R. England, D.J. Vaughan. Transformation of synthetic mackinawite to hexagonal pyrrhotite: a kinetic study. *American Mineralogist*, **80**(9–10), 960–967 (1995).

[4] J.L. Jambor, D.W. Blowes. Theory and applications of mineralogy in environmental studies of sulphide bearing mine waste. In *Modern Approaches to Ore and Environmental Mineralogy*, L.J. Cabri, D.J. Vaughan (Eds.), Min Soc of Canada Short Course Series 27, pp. 367–401 (1998).

[5] M.T. Dove, M. Calleja, J. Wakelin, K. Trachenko, G. Ferlat, P. Murray-Rust, N.H. de Leeuw, Z. Du, G.D. Price, P.B. Wilson, J.P. Brodholt, M. Alfredsson, A. Marmier, R.P. Tyer, L.J. Blanshard, R.J. Allan, K. K. van Dam, I.T. Todorov, W. Smith, V.N. Alexandrov, G.J. Lewis, A. Thandavan, S.M. Hasan. Environment from the molecular level: an escience testbed project. *Proceedings of UK e-Science All Hands Meeting 2003*, pp. 302–305, (2003), (EPSRC, ISBN 1-904425-11-9).

[6] M. Calleja, R. Bruin, M.G. Tucker, M.T. Dove, R.P. Tyer, L.J. Blanshard, K.K. van Dam, Robert J. Allan, C. Chapman, W. Emmerich, P.B Wilson, J.P. Brodholt, A. Thandavan, V.N. Alexandrov. Collaborative grid infrastructure for molecular simulations: The eMinerals minigrid as a prototype integrated compute and data grid. *Molecular Simulations* (in press).

[7] L.J. Blanshard, K. Kleese, M.T. Dove. Environment from the molecular level e-science project and its use of CLRC's web services based data portal. *Proceedings of the First International Conference on Web Services*, pp. 164–167, (2003), (CSREA Press, ISBN 1-892512-40-8).

[8] L. Blanshard, R. Tyer, M. Calleja, K. Kleese, M.T. Dove. Environmental molecular processes: management of simulation data and annotation. *Proceedings of the UK e-Science All Hands Meeting 2004*, pp. 637–644, (2004), (ISBN 1-904425-21-6).

[9] M. Calleja, L. Blanshard, R. Bruin, C. Chapman, A. Thandavan, R. Tyer, P. Wilson, V. Alexandrov, R.J. Allen, J. Brodholt, M.T. Dove, W. Emmerich, K.K. van Dam. Grid tool integration within the eMinerals project. *Proceedings of the UK e-Science All Hands Meeting*, pp. 812–817, (2004), (ISBN 1-904425-21-6).

[10] P. Martin, G.D. Price, L. Vocadlo. An *ab initio* study of the relative stabilities and equations of state of FeS polymorphs. *Mineral. Mag.*, **65**(2), 181–191 (2001).

[11] H.E. King, C.T. Prewitt. High-pressure and high-temperature polymorphism of iron sulphide (FeS). *Acta Crystallogr. B*, **38**, 1877–1887 (1982).

[12] D. Hobbs, J. Hafner. Magnetism and magnetostructural effects in transition-metal sulphides. *J. Phys. Condens. Matter.*, **11**, 8197–8222 (1999).

[13] A. Rohrbach, J. Hafner, G. Kresse. Electronic correlation effects in transition-metal sulphides. *J. Phys. Condens. Matter*, **15**, 979–996 (2003).

[14] J.P. Rueff, C.C. Kao, V.V. Struzhkin, J. Badro, J. Shu, R.J. Hemley, H.K. Mao. Pressure-induced high-spin to low-spin transition in FeS evidenced by X-ray emission spectroscopy. *Phys. Rev. Lett.*, **82**, 3284–3287 (1999).

[15] K. Kusaba, Y. Syono, T. Kikegawa, O. Shimomura. Structure of FeS under high pressure. *J. Phys. Chem. Solids*, **58**, 241–246 (1997).

[16] G. Kresse, J. Furthmuller. Efficient iterative schemes for *ab initio* total-energy calculations using a plane-wave basis set. *Comput. Mater. Sci.*, **6**, 15–50 (1996).

[17] S.H. Vosko, L. Wilk, M. Nussair. *Can. J. Phys.*, **58**, 1200 (1980).

[18] M. Methfessel, A.T. Paxton. High precision sampling for Brillouin-zone integration in metals. *Phys. Rev. B.*, **40**, 3616–3621 (1989).

[19] H.J. Monkhorst, J.D. Pack. Special points for Brillouin-zone integration. *Phys. Rev. B*, **13**, 5188–5191 (1976).